

Insights into amine-based CO₂ capture: an ab initio self-consistent reaction field investigation

Phil Jackson · Ariana Beste · Moetaz Attalla

Received: 28 May 2010 / Accepted: 17 December 2010 / Published online: 30 December 2010
© The Author(s) 2010. This article is published with open access at Springerlink.com

Abstract Ab initio many-body perturbation theory (MP2/6-311++G(dp)), density functional theory (B3LYP/6-31++G(d,p)) and self-consistent reaction field (IEF-PCM UA HF/6-31G(d)) calculations have been used to study the CO₂ capture reagents NH₃, 2-hydroxyethylamine (MEA), diaminoethane (EN), 2-amino-1-propanol (2AIP), diethanolamine (DEA), *N*-methyl-2-hydroxyethylamine (*N*-methylMEA), 2-amino-2-methyl-1-propanol (AMP), trishydroxymethylaminomethane (tris), piperazine (PZ) and piperidine (PD). This study involved full conformational searches of the capture amines in their native and protonated forms, and their carbamic acid and carbamate derivatives. Using this data, we were able to compute Boltzmann-averaged thermodynamic values for the amines, carbamates and carbamic acid derivatives, as well as equilibrium constants for a series of ‘universal’ aqueous capture reactions. Important findings include (i) relative p*K*_a values for the carbamic acid derivatives are a useful measure of carbamate stability, due to a particular chemical resonance which is also manifest in short computed N–CO₂H bonds at both levels of theory, (ii) the computational results for sterically hindered amines such as AMP and tris are consistent with these species forming carbamates which readily hydrolyse

and (iii) the amine-catalysed reaction between OH[−] and CO₂ to generate bicarbonate correlates with amine p*K*_a. Thermodynamic data from the ab initio computations predicts that the heterocycles PD and PZ and the acyclic sorbent EN are good choices for a capture solvent. AMP and tris perform poorly in comparison.

Keywords Post-combustion capture · Amine · Ab initio · Piperazine · Alkanolamine

Introduction

Anthropogenic CO₂ emissions must be reduced over the coming decades in order to avoid climate change. To minimize global environmental impacts, atmospheric CO₂ needs to be stabilized at a level less than or equal to 450 ppm [1], which should limit average global temperature rises to less than 2 °C. To achieve such emission reductions, technologies such as solvent-based post-combustion carbon capture (PCC), which can be retro-fitted to existing coal-fired electricity generators, have to be developed and deployed within a relatively short time frame. Now that greenhouse gas emissions from developing nations have finally surpassed those of developed nations [2], there is an even greater imperative for CO₂ capture to succeed. Currently, the large-scale roll-out of solvent-based PCC is hampered by economic factors, which are a deterrent for owners of generator infrastructure (e.g., PCC plant capital and solvent on-costs, see below), and government coercion via emission trading schemes will be widely used to stimulate uptake [3].

Aside from economics, a further impediment to the immediate deployment of PCC is the flue gas scrubbing performance of alkanolamine capture solvents. Whereas a

Electronic supplementary material The online version of this article (doi:10.1007/s11224-010-9719-2) contains supplementary material, which is available to authorized users.

P. Jackson · M. Attalla (✉)
Coal Portfolio, CSIRO Energy Centre, 10 Murray-Dwyer
Circuit, Mayfield West, NSW 2304, Australia
e-mail: moetaz.attalla@csiro.au

A. Beste
Computational Chemical Sciences Group,
Oak Ridge National Laboratories, PO Box 2008
MS6367, Oak Ridge, TN 37831-6367, USA

number of solvents can efficiently remove acid gases (CO_2 , SO_2) from natural and industrial gas streams at higher pressures (>5 bar), the lower pressures typical of coal-fired power station flue gas streams pose separate difficulties. Problems may also be encountered for individual CO_2 scrubbing solvents, such as monoethanolamine (MEA) and piperazine (PZ), the former being prone to oxidation by flue gas components [4, 5], whereas the latter is a secondary amine that can react with NO_x -containing flue gas to form hazardous nitrosamines [6], [7, p. 1100].

As part of an experimental program within the CSIRO organization, more than 70 organic amines have been screened as potential CO_2 capture solvents. This work has been carried out over a two and a half year period, with several dedicated technicians performing the experiments; these have included various kinetics studies (chemometric modelling [8], nuclear magnetic resonance spectroscopy [9], thermogravimetric analysis [10] and Fourier transform infrared spectroscopy [11]) as well as loading or capacity measurements [12]. In addition, many of the CO_2 capture candidates were also synthesized in-house, at significant cost. After completion of the laboratory investigations, promising candidates were synthesized in bulk for further lab-scale trials, and—contingent on scale-up performance tests—for deployment at one of several pilot-scale PCC plants located at regional power-generating infrastructure [13].

These laboratory studies have been useful for identifying “high performers” amongst a broad suite of alkanolamines, however, our understanding of the properties that confer excellent capture characteristics are still only rudimentary. There are inherent difficulties in deriving experimental thermodynamic values, i.e., reactions cannot be studied with laboratory techniques in isolation, due to the interplay of numerous solvent equilibria, and several capture products and intermediates are unstable under capture conditions. This means that measurement uncertainty could be greater than 50% of the experimental value. A knowledge of accurate thermochemical values is one key to lowering overall PCC costs.

To fast-track our research efforts, a first principles investigation of a representative amine subset has been undertaken using density functional theory and many-body techniques. The primary goal of this study is the rapid identification of proven high-performing CO_2 capture candidates, however, we also stand to gain a deeper understanding of the structural features that impart desirable capture properties. After computing gas phase reaction energies and polarizable continuum model free energies of solvation (for a recent review of this methodology, see: [14]), aqueous equilibrium constants have been obtained via the use of thermodynamic cycles. A thorough investigation of the conformational spaces of the amines,

protonated amines, and their carbamate- and carbamic acid-derivative was undertaken in order to predict trends for future studies of more complex alkanolamine candidates. Relative carbamate stability has been successfully studied previously [15] using computational techniques. Typically, the time and expense incurred with the generation of this data is low compared to the in-house experimental efforts expended to date.

Computational method

Gas phase calculations at the B3LYP/6-31++G(d,p) and MP2/6-311++G(d,p) levels were performed using the GAMESS Revision 1 software package [16]. GAMESS employs a B3LYP functional formula based on the VWN5 local correlation functional, which may differ from other B3LYP implementations [17]. The MacMolPlt 7.0 program [18] was used for visualization.

Geometry optimizations were performed using a Newton–Raphson steepest descent algorithm until a stationary point was located, characterized by a gradient less than 0.0001. We have used the recommended density of grid points to reduce integration errors in the DFT exchange–correlation quadrature to less than 1 microhartree per atom, namely $\text{NRAD} = 96$, $\text{NTHE} = 36$ and $\text{NPHI} = 72$, producing 248832 grid points per atom. Vibrational analysis was performed for all stationary points.

Molar heat capacities (C_p , C_v), entropies, enthalpies and free energies at specified temperatures for both molecules and ions were provided by the GAMESS program. These values were scaled using factors proposed by Scott and Radom [19]. All gas phase reaction energies were calculated according to thermochemical conventions [20]. The hybrid DFT functional B3LYP was selected for its reliability and widespread chemical application [21], in addition to MP2 calculations.

The integral equation formalism-polarizable continuum model (IEF-PCM UA HF/6-31G(d)) [14, 22] was used for the calculation of solvation free energies, from which reaction energies for both the MP2 and DFT values in the solution phase could be derived. The total free energy of solvation is expressed [23]:

$$\Delta G_{\text{soln}} = G_{\text{el}} + G_{\text{cav}} + G_{\text{disp}} + G_{\text{rep}} \quad (1)$$

where ‘el’, ‘cav’, ‘dis’ and ‘rep’ represent electrostatic, cavitation, dispersion and repulsion contributions, respectively. The usual parameters for water, i.e., dielectric constant $\epsilon = 78.39$, solvent radius ($\text{H} = 1.2 \text{ \AA}$, $\text{O} = 1.5 \text{ \AA}$) and solvent molecule density per unit volume (0.03348 \AA^3), were used to define the continuum.

Within the PCM (UAHF) framework, ΔG_{soln} is derived using a HF/6-31G(d) gas phase structure. Reasonably good

agreement was found between experimental and calculated ΔG_{soln} values for small ions and molecules involved in the capture chemistry process (see Table S1, Supporting information). The IEF-PCM UA HF/6-31G(d) calculations were all performed with the Gaussian 03 package [24]. Using thermodynamic cycles and gas phase free energies, aqueous free energies of reaction for capture processes of interest were evaluated. $\text{p}K_{\text{a}}$ values for amines and carbamic acids were also generated from first principles using the free energy data according to the method outlined by Tomasi and co-workers [25], and the results compared and discussed.

In order to evaluate amine capture performance, reactions central to the aqueous CO_2 capture process need to be selected. We calculated K_{eq} for the following aqueous equilibria, which are widely considered universal for CO_2 capture by primary and secondary amines (Scheme 1).

Equilibria 1 and 5 are acid–base equilibria, 2 and 4 are CO_2 fixation (carbon capture) equilibria, and 3 is the carbamate/bicarbonate equilibrium (carbamate hydrolysis). Equilibrium 5 only plays a minor role according to the experimental K_{eq} (298): $\text{HCO}_3^- + \text{OH}^- \rightleftharpoons \text{CO}_3^{2-} + \text{H}_2\text{O}$, 2.175×10^{-4} [26] and is ignored for the purposes of this study. According to the results of Truhlar and co-workers [27] and Goddard and co-workers [28], the ion free energies of solvation will be the major source of error for the solution phase thermochemistry. We refrain from applying cluster pairs, mixed cluster/continuum models or addition of explicit water molecules to improve the ion solvation values, and instead focus on inter-amine trends. For the IEF-PCM continuum method, the addition of explicit water molecules can lead to even larger errors [29]. The free energy of solvation of water molecule predicted by the IEF-PCM UAHF/6-31G(d) method was found to be -25.8 kJ/mol. This does not appear to include the free energy correction for the change of state ($+7.9$ kJ/mol) [28], so a revised value $\Delta G_{\text{soln}}(\text{H}_2\text{O}) = -17.9$ kJ/mol was used throughout.

The capture amine subset we have investigated includes the primary amines NH_3 , 2-hydroxyethylamine (MEA), diaminoethane (EN) and 2-amino-1-propanol (2A1P); the secondary amines diethanolamine (DEA) and *N*-methyl-2-

hydroxyethylamine (*N*-methylMEA); the sterically hindered primary amines 2-amino-2-methyl-1-propanol (AMP) and tris(hydroxymethyl)aminomethane (tris); and finally, the heterocycles piperazine (PZ) and piperidine (PD).

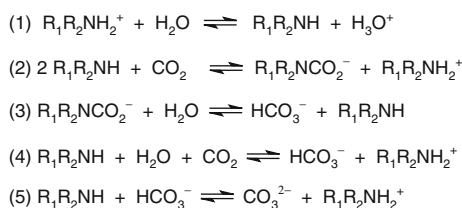
Results and discussion

The veracity of our approach has been assessed by determining selected gas phase thermochemistry (basicities, proton affinities) for a set of simple organic amines which includes ammonia, methylamine, dimethylamine, ethylamine, methylethylamine, propylamine and trimethylamine. Ammonia is included as it finds application as a CO_2 capture solvent, however, the alkylamines are considered too volatile for PCC application. Gas phase proton exchange equilibria, notably gas phase basicities, are related to solution phase $\text{p}K_{\text{a}}$ values by solvation free energies. The performance of B3LYP and MP2 in predicting gas phase basicities is thus important for the prediction of equilibrium constants. Alkylamines are simple monofunctional amine molecules for which these values can be rapidly computed and compared with accurate experimental values. The results are shown in Table S2 of the supporting information section. Both levels of theory succeed in predicting the correct order for the gas phase basicities (GB) and proton affinities (PA). The overall theoretical trend is to overestimate both values, with the mean unsigned errors (MUEs) for the MP2 results (PA 10.1 kJ/mol, GB 15.1 kJ/mol) being approximately twice as large as the B3LYP MUEs (PA 4.0 kJ/mol, GB 8.4 kJ/mol).

The corresponding PAs and GBs for the set of capture amines being investigated are given in Table 1. We observe that the cyclized structures of MEA and EN are preferred over their extended counterparts in the gas phase. Studies by Bouchoux [30] and Karpas [31] have confirmed the importance of hydrogen bonding in polyfunctional molecules when calculating gas phase basicities and proton affinities.

For an explanation of the nomenclature used to describe the orientation of substituents attached to the ring heteroatoms of PD and PZ, see Scheme 2. Our calculations indicate that the chair conformers of neutral and protonated PZ and PD are present in the experiments, consistent with the literature [32]. Less than 4 kJ/mol separates *eq*(H)–PD and *ax*(H)–PD, *eq*(H)*eq*(H)–PZ and *eq*(H)*ax*(H)–PZ. For PD, the experimental *eq*–*ax* energy separation for the chair conformers is 2.1 kJ/mol [33], a value that compares well with MP2 (4.1 kJ/mol) and B3LYP (3.0 kJ/mol) results.

Concerning heterocycle thermochemistry, the theoretical gas phase PA's are well within the accuracy of the methods: for PD, $\text{PA}_{\text{MP2}} = 959.1$ kJ/mol, $\text{PA}_{\text{B3LYP}} = 958.7$ kJ/mol, $\text{PA}_{\text{expt}} = 954.0$ kJ/mol [20]; for PZ, $\text{PA}_{\text{MP2}} = 953.4$ kJ/mol,



Scheme 1 Universal reaction equilibria for CO_2 capture by aqueous amines. R_1 and/or $\text{R}_2 = \text{H}, \text{CH}_2\text{OH}, \text{C}_2\text{H}_4\text{OH}, \text{etc}$

Table 1 Theoretical and experimental gas phase basicities and proton affinities for organic amines used in CO₂ capture

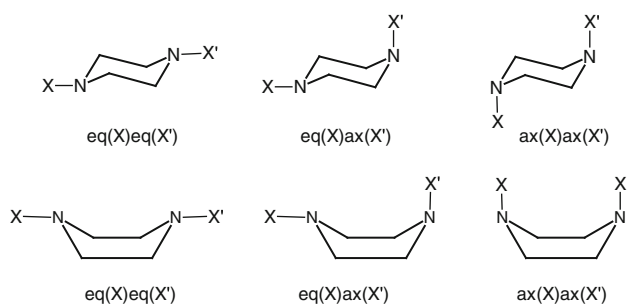
Alkanolamine	Proton affinity (kJ/mol)					Gas phase basicity (kJ/mol)				
	Theory		Expt ^b	UE ^c		Theory		Expt ^b	UE ^c	
	MP2	B3LYP		MP2	B3LYP	MP2	B3LYP		MP2	B3LYP
MEA										
Extended	905.6	901.4				881.1	876.6		–	–
H-bonded	930.3	926.2	930.3	0.0	4.1	901.6	896.4	896.8	4.8	0.4
DEA										
Extended	937.5	931.7	–	–	–	915.4	909.7			–
H-bonded ^a	981.2	978.2	953.0	28.2	25.2	954.7	950.1	920.0	34.7	30.1
EN										
Extended	911.2	909.2				885.3	883.4			
H-bonded	960.5	958.0	951.6	8.9	6.4	929.4	927.1	912.5	16.9	14.6
PZ										
Chair	953.4	953.0	943.7	9.7	9.3	924.2	923.9	914.7	9.5	9.2
Boat	966.6	963.7				936.7	933.8			
PD										
Chair	959.1	958.7	954.0	5.1	4.7	930.1	929.6	921.0	9.1	8.6
Boat	961.2	961.0				932.2	931.6			

The values were derived using the lowest energy cyclized and extended conformers

^a See text for discussion

^b Experimental values from [20]

^c Unsigned error



Scheme 2 Notation used to describe substituent orientation on ring heteroatoms

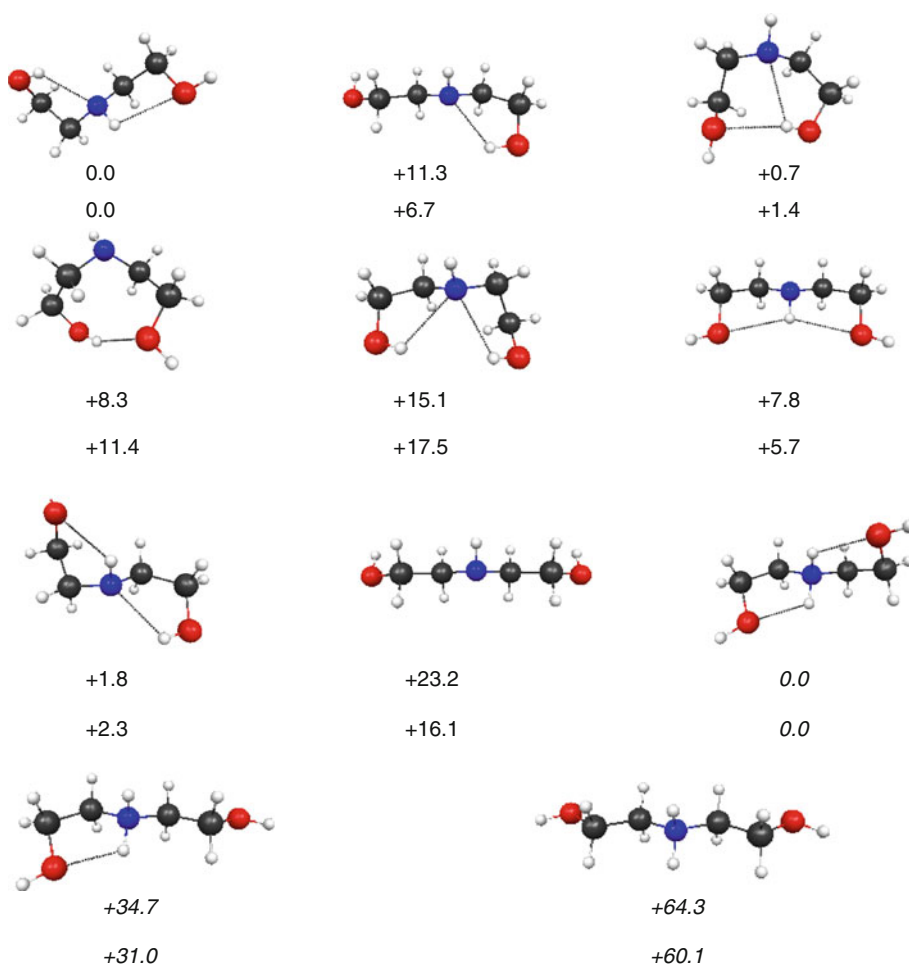
$PA_{B3LYP} = 953.0$ kJ/mol, $PA_{\text{expt}} = 943.7$ kJ/mol [20]. The theoretical GB values fare a little worse, with MUE's nearing 10 kJ/mol.

The major discrepancies in Table 1 occur for the proton affinity and gas phase basicity for DEA. Assuming that DEA and $DEAH^+$ will also adopt hydrogen-bonded structures in the gas phase, using the lowest energy cyclized conformers to evaluate thermochemical values leads to overestimation of PA by 28.2 (MP2) and 25.2 (B3LYP) kJ/mol, and GB by 34.7 (MP2) and 30.1 (B3LYP) kJ/mol. This has been noted previously [34]. The experimental values were determined using fast atom bombardment-mass spectrometry (FAB-MS) with binary

mixtures. The formation of proton-bridged dimers during ionization has been offered as a possible explanation for the discrepancy between theory and experiment. All conformers located for DEA and $DEAH^+$ are shown in Fig. 1. For neutral DEA, there are several conformers within 10 kJ of the global minimum. Much larger energy differences are predicted for $DEAH^+$, as the N-centred hydrogens interact more strongly with the R–OH oxygen lone pairs.

If it is assumed that the $DEAH^+$ conformers are *not* in equilibrium, there is good correspondence between experiment and theory if the conformer lying 34.7 and 31.0 kJ/mol (at the MP2 and B3LYP levels, respectively; see Fig. 1) above the global minimum is used in the calculation of the gas phase properties. The results obtained are: $PA_{MP2} = 946.4$ kJ/mol, $PA_{B3LYP} = 947.2$ kJ/mol, $PA_{\text{expt}} = 953.0$ kJ/mol; $GB_{MP2} = 924.5$ kJ/mol, $GB_{B3LYP} = 920.1$ kJ/mol, $GB_{\text{expt}} = 920.0$ kJ/mol. These differences between experimental and theoretical values are consistent with the magnitude of the unsigned errors obtained for MEA, and suggest that the lowest energy conformer of $DEAH^+$ is not formed in the FAB ion source. A point noted by Kebarle and coworkers is that the experimental method does not take into account entropy changes associated with cyclization upon protonation ($\Delta G_r \cong \Delta H_r$) [35]. When this is considered for the higher energy $DEAH^+$ conformer, good agreement between experiment and theory is once again obtained.

Fig. 1 Minima located during conformational searches of the DEA and DEAH⁺ surfaces at the MP2/6-311++G(d,p) and B3LYP/6-31++G(d,p) levels. Relative energies (with respect to the lowest energy conformer) are also given (MP2 top, B3LYP bottom). DEAH⁺ relative energies are italicized. *White* = hydrogen; *black* = carbon; *red* = oxygen; *blue* = nitrogen. *Dashed line* = hydrogen bond



Carbamate and carbamic acid derivatives of organic amines used in CO₂ capture

Both the *syn*- and *anti*-variants of the acid derivatives of acyclic sorbent molecules have been extensively investigated, covering all hydrogen bonding possibilities, as well as all conformers of the corresponding carbamates. As examples, the various minima located for bis(2-hydroxyethyl) carbamate and bis(2-hydroxyethyl) carbamic acid, the CO₂ capture products of DEA, are shown in Fig. 2, while the results for the difunctional sorbent AMP (2-amino-2-methyl-1-propanol) are shown in Fig. 3.

The results for the hydrogen-bonded conformers of the acyclic carbamic acids establishes that hydrogen bonding between the R–OH proton and the carbonyl oxygen of the –COOH group confers gas phase stability. Globally, a *syn*-acid group proton also confers stability. This is attributed to the chemical stabilization shown in Scheme 3.

Evidence for the stabilization in Scheme 3 can be found in the carbamic acid N–C bond lengths, which are intermediate between C–N single bond (e.g., carbamate bond lengths) and C=N double bond lengths, e.g., ethanimine, see Table 2.

Another well known analogue with which comparisons can be drawn is the amide bond, which is semi-rigid, due to the partial double bond character of the N–C bond adjacent to the carbonyl. A manifestation of the shortened N–C bond in the carbamic acid group is the reduced gas phase acidity of the –COOH proton (discussed *vide infra*). There is also evidence for this effect in crystals of a solid complex derived from CO₂/PD vapour [35].

As is the case for underivatized heterocycles PD and PZ, their carbamate derivatives can—in principle—adopt different structural conformations as a result of (i) ring puckering at the 1- and 4-position and (ii) N–X group orientations at the heteroatom (either axial or equatorial). Chair forms of carbamic acid and carbamate are once again energetically preferred for both heterocycles at both levels of theory, and discussion of boat conformations is not warranted. For the carbamate derivative of PD, MP2 favours *ax*(CO₂) group orientation by 19 kJ/mol, whereas B3LYP slightly favours the *eq*(CO₂) conformer (by 3.5 kJ/mol). This marks the first real theoretical discrepancy between B3LYP and MP2.

For the carbamic acid derivative of PD, MP2 slightly favours the *ax*(CO₂H) orientation by 2.2 kJ/mol, whereas at

Fig. 2 Minima located during conformational space searches of the DEA CO₂ capture products bis(2-hydroxyethyl)carbamic acid (*top and centre rows*) and bis(2-hydroxyethyl)carbamate (*bottom row*) at the MP2/6-311++G(d,p) and B3LYP/6-31++G(d,p) levels. With the exception of the conformer in the middle row at centre (*anti-*), all acid conformers are *syn* with respect to the configuration of the acid group proton. Relative energies (with respect to the lowest energy conformer) are also given (MP2 *top*, B3LYP *bottom*). White = hydrogen; black = carbon; red = oxygen; blue = nitrogen. Dashed line = hydrogen bond. *Imaginary frequency of 35.4i cm⁻¹ at this level of theory

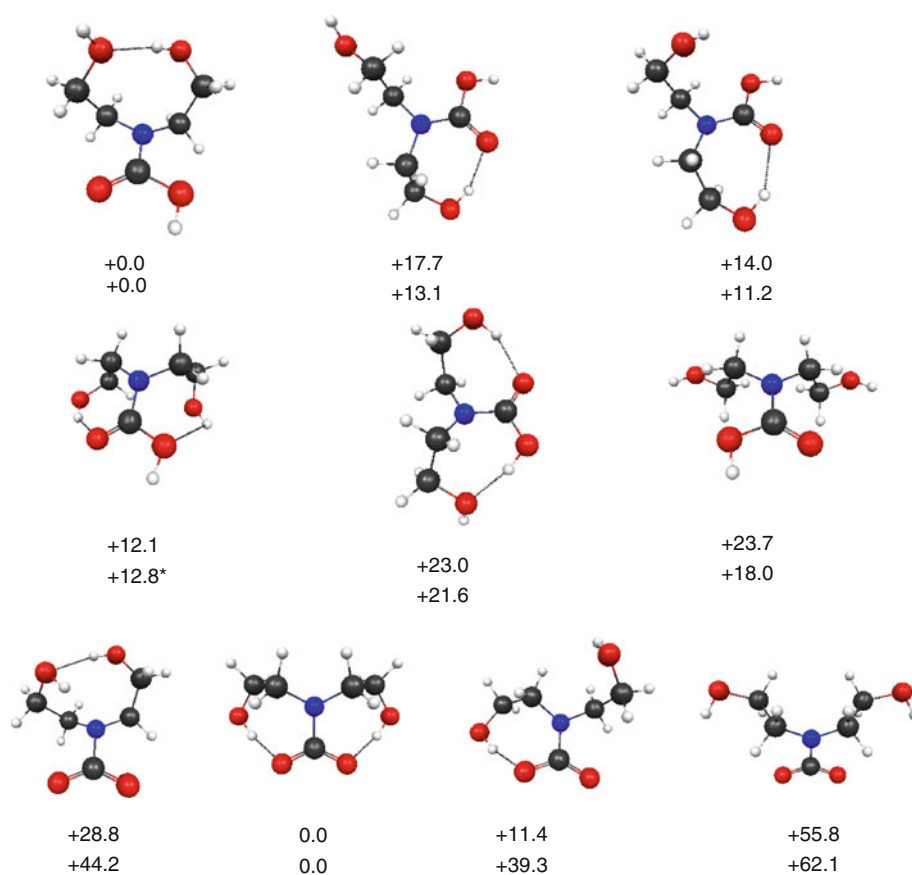
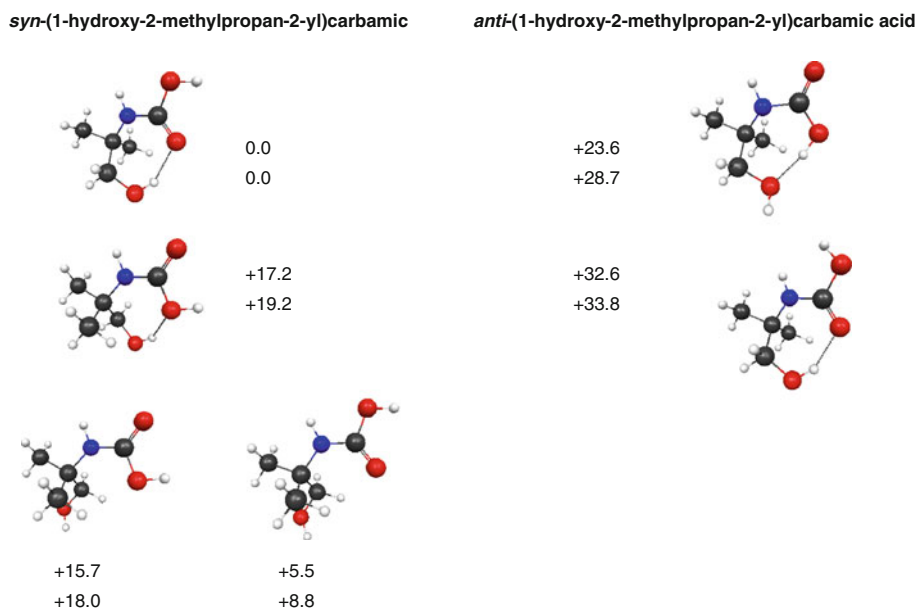


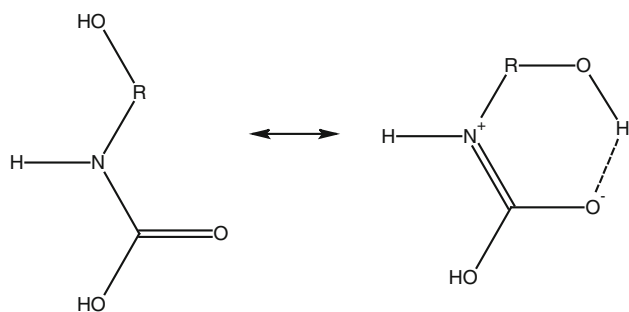
Fig. 3 Structures and relative energies (MP2 *top*, B3LYP *bottom*) of the gas phase *syn*- and *anti*-conformer of (1-hydroxy-2-methylpropan-2-yl)carbamic acid, the AMP CO₂ capture product



the B3LYP level, there is near-planarity at the N-centre (the dihedral angle between the C(2)–N=C=O(OH) and C(6) is $\sim 171^\circ$, see discussion *vide infra*). The B3LYP minimum is *eq*(CO₂H), and *ax*(CO₂H) conformers were found to collapse to the equatorial form, even when an augmented triple-zeta basis was used in the geometry optimization. Hessian

analysis for the *ax*(CO₂H) acid derivative of PD (dihedral angle 171°) at the B3LYP/6-31++G(d,p) level revealed a small imaginary frequency of 56i cm⁻¹ associated with atomic motions leading to the *eq*(CO₂H) conformer.

For PZ acid and carbamate derivatives, the MP2 calculations suggest less than 4 kJ/mol separates the various



Scheme 3 Hydroxyalkylcarbamic acid stabilization gained via intramolecular hydrogen bonding

eq-ax combinations of the carbamate, and less than 6 kJ/mol for the carbamic acids. MP2 slightly favours the *eq(CO₂)ax(H)* carbamate and the *ax(CO₂H)ax(H)* acid conformers. Less than 8 kJ/mol separates the carbamate isomers at the B3LYP level, and any barrier between the *ax(CO₂)ax(H)* and the most stable *eq(CO₂)ax(H)* carbamate isomers is negligibly small. Only acid conformers with *eq(CO₂H)* groups could be located at the B3LYP/6-31++G(d,p) level, and the *eq(CO₂H)eq(H)* isomer is preferred by 3.5 kJ/mol.

For the carbamic acid derivatives of the heterocycles, it is unclear if B3LYP is overestimating the planarity of the N-centre or if MP2 is underestimating this. This could be a limitation of the theory, as hessian analysis for the lowest energy piperazine derivatives *ax(H)ax(CO₂H)* and *eq(H)ax(CO₂H)* at the B3LYP level (C2–N1–C7–C6 dihedral angles of 171.1° and 166.2°, respectively) revealed no imaginary frequencies. As ΔG_{soln} values did not change appreciably with conformational changes at the heteroatoms, only the most stable gas phase conformers

were used to evaluate ΔG_{aq} for the carbamate/carbamic acid species.

A single *anti* boat conformer of piperazine carbamic acid was investigated using B3LYP (*anti-eq(CO₂H)ax(H)*), which was found to be more than 50 kJ/mol less stable than the lowest energy *syn-eq(CO₂H)eq(H)* chair conformer, so *anti* conformers were not investigated further.

The notion of stable zwitterions for the carbamic acid derivatives of the reagents EN and PZ has also been investigated. Both zwitterions are expected to be important in condensed phase chemistry, however, investigations in the gas phase revealed the zwitterion $^+\text{H}_3\text{N}-\text{C}_2\text{H}_4-\text{NHCO}_2^-$ is unstable to rearrangement (to an *anti-acid* conformer). Charge separation stabilizes the zwitterion form of PZ-carbamic acid, which is a minimum at both levels of theory, but is much less stable in the gas phase than *syn-acid* forms (free energy differences, lowest *syn*-form and zwitterion form: $E_{\text{B3LYP}} = +181.1$ kJ, $E_{\text{MP2}} = +182.1$ kJ).

Free energies of solvation

The IEF-PCM UA HF/6-31G(d) solvation free energies (ΔG_{soln}) of some simple molecules and ions implicated in solvent-based CO₂ capture are shown in Table S2, supporting information. The best results are obtained for neutral species, while the results for the anions are slightly worse. Of these, the discrepancy between the experimental and theoretical ΔG_{soln} is largest for OH[−] at 16.5 kJ/mol (this analysis excludes a comparison of the results for HCO₃[−], for which the experimental value is an estimate). The paucity of experimental data for ion ΔG_{soln} values limits our capacity to critically assess these values, so emphasis throughout is placed on relative, rather than

Table 2 N–C bond lengths of the carbamate and carbamic acid derivatives of the CO₂ capture amine subset investigated

Sorbent molecule	Carbamic acid N–C(O)OH bond length (Å)		Carbamate N–C(O)O [−] bond length (Å)	
	MP2/6-311++G(d,p)	B3LYP/6-31++G(d,p)	MP2/6-311++G(d,p)	B3LYP/6-31++G(d,p)
Ethanimine	1.280	1.280		
MEA			1.468	1.476
Derivatives				
Ammonia	1.364	1.366	1.465	1.469
2A1P	1.348	1.353	1.450	1.446
AMP	1.349	1.353	1.450	1.445
MEA	1.349	1.354	1.447	1.445
EN	1.356	1.360	1.463	1.452
DEA	1.355	1.361	1.437	1.434
N-MethylMEA	1.348	1.354	1.453	1.449
PD	1.361	1.360	1.476	1.471
PZ	1.362	1.361	1.482	1.473
Tris	1.347	1.352	1.453	1.448

The N–C bond lengths of MEA (C–N single bond) and ethanimine (C=N) are included for reference

absolute, computed free energies and equilibrium constants (see below). It is well established that values for neutral species are slightly more accurate than values for ions as a result of the limited experimental data set which were used in model parametrization [22].

The magnitudes of the computed ΔG_{soln} of the alkanolamines suggests (i) orienting polarized hydrogen atoms (bonded to either N or O atoms) towards the solvent surface, i.e., maximizing electrostatic interactions between the polarized solvent and solute, leads to larger negative values, and (ii) intramolecular hydrogen bonding (occluding polarized hydrogen atoms) leads to smaller negative values. Selected results for ΔG_{soln} of extended and intramolecularly hydrogen-bonded alkanolamines, and their protonated analogues, are shown in Table 3. Alkanolamines with a single R–OH group can form a single intramolecular hydrogen bond with the amino centre; the difference between the ΔG_{soln} of this group for the hydrogen-bonded and extended forms (~ 7 – 9 kJ/mol, the approximate hydrogen bond strength in the gas phase) suggests there will be only a small energetic difference between the two forms in the solution phase, as the gas phase hydrogen bonding stabilization is largely cancelled by a smaller negative ΔG_{soln} value (see below).

For the neutral and protonated heterocycles, more negative ΔG_{soln} are observed when the hydrogens attached to the nitrogen atoms are in axial conformations; equatorial N–H atoms give rise to ΔG_{soln} values a few kJ/mol less negative than their axial counterparts. The overall ring conformation appears to have little effect on the ΔG_{soln} values.

According to Marcus [36], large negative ΔG_{soln} values lead to solutions of higher viscosity, as ordered solutions

are formed and there is little disturbance to the bulk water structure beyond the first few solvation shells. From an engineering perspective, this is an undesirable solvent attribute, as this will reduce solvent “pockets” for dissolved gases. Ideally, a good capture solvent (in its native or unreacted form) should have a small negative ΔG_{soln} , however, there is a trade-off between reduced viscosity and solvent volatility, as both of these quantities are represented to various extents in the ΔG_{soln} values. For the acyclic hydrogen-bonded candidates, AMP appears to be the solvent of choice for reduced viscosity. In the protonated form, it also has the least negative ΔG_{soln} value, suggesting less favourable solute–solvent interactions. The best choices, according to the ΔG_{soln} values, would be PD or ammonia. The low ΔG_{soln} value for ammonia underscores its small molecular size and high volatility, a major difficulty associated with its deployment as a capture solvent. PD is the best choice based on ΔG_{soln} values, but again it is the most volatile of the organic amines.

All reaction enthalpies, free energies and equilibrium constants were derived with solution-averaged total energies (see Table 4).

Reaction free energies and related thermodynamic values derived from quantum calculations

pK_a values

Computed pK_{a} values for some members of the capture amine subset have been presented previously [37]. Theoretical pK_{a} values for the capture amines decrease in the

Table 3 IEF-PCM UA HF/6-31G(d) solvation energies for extended and intramolecularly hydrogen-bonded conformers of selected neutral and protonated organic amines used in solvent-based CO₂ capture

Alkanolamine	Solvation free energies (kJ/mol)					
	Neutral form			Protonated form		
	Extended or <i>eq</i> -H	H-bonded or <i>ax</i> -H	Absolute difference	Extended or <i>eq</i> -H	H-bonded or <i>ax</i> -H	Absolute difference
2A1P	−40.5	−31.7	8.9	−296.3	−273.6	22.6
AMP	−35.6	−28.3	7.7	−278.0	−256.6	21.5
MEA	−44.2	−35.0	9.2	−315.3	−288.9	26.4
DEA ^a	−66.2	−48.8	17.3	−315.5	−264.9	50.6
DEA ^b		−57.2	9.0		−288.8	26.7
PD chair	−20.9	−23.2	2.3	−259.5 ^c	−258.6 ^c	0.9
PD boat	−20.1	−23.1	3.0			
PZ chair ^d	−41.8	−47.1	5.3	−290.7	−300.6	9.9
PZ boat ^d	−45.2	−47.7	2.5	−279.4	−298.8	19.4

^a Results for lowest energy conformers with two intramolecular H-bonds

^b Results for lowest energy conformers with a single intramolecular H-bond

^c Difference between chair ‘a’ and boat ‘b’ forms

^d For the neutrals, *eq*-H corresponds to *eq*-H *eq*-H conformer, *ax*-H corresponds to *ax*-H *ax*-H conformer

Table 4 Total solution energies (Boltzmann-averaged) at 298.15 K for amine sorbents and derivatives used in the calculation of reaction enthalpies, free energies and equilibrium constants

	Energies (Hartree)			
	M	M + H ⁺	M-CO ₂ ⁻	MCO ₂ H
Sorbent/MP2				
NH ₃	-56.4075359	-56.8558695	-244.1747652	-244.6186717
2A1P	-248.9914429	-249.4380958	-436.7602990	-437.2082897
AMP	-288.1687894	-288.6130131	-475.9336754	-476.3819063
MEA	-209.8169222	-210.2646833	-397.5859438	-398.0322586
EN	-189.9483509	-190.4015172	-377.7161836	-378.1650720
DEA	-363.2313360	-363.6841211	-551.0061739	-551.4438515
N-MethylMEA	-248.9762912	-249.4269019	-436.7425401	-437.1907863
PD	-251.0711270	-251.5240561	-438.8373711	-439.2857453
PZ	-267.1063211	-267.5607662	-454.8741741	-455.3260018
Tris	-438.3287172	-438.7756834	-626.0963432	-626.5396010
Sorbent/B3LYP				
NH ₃	-56.5319381	-56.9762998	-244.6407795	-245.0827984
2A1P	-249.5301721	-249.9747958	-437.6340044	-438.0832191
AMP	-288.796096	-289.2402884	-476.8993801	-477.3435147
MEA	-210.2627685	-210.7082837	-398.3714073	-398.8160523
EN	-190.375506	-190.8268854	-378.4813247	-378.9298160
DEA	-363.9948339	-364.4456305	-552.0969826	-552.5407112
N-MethylMEA	-249.5180626	-249.9662303	-437.6216191	-438.0682160
PD	-251.6568412	-252.1094577	-439.7595585	-440.2064883
PZ	-267.7079615	-268.1622482	-455.8117101	-456.2634354
Tris	-439.2093993	-439.6562648	-627.3132031	-627.7525924

Values given in Hartree

order (most basic to least basic), *MP2*: PZ > EN > PD > DEA > *N*-methylMEA > NH₃ > MEA > tris > 2A1P > AMP; *B3LYP*: PZ > PD > EN > DEA > *N*-methylMEA > tris > MEA > 2A1P > NH₃ > AMP; *Expt*: PD > EN > PZ > *N*-methylMEA > AMP > MEA > NH₃ > DEA [38]. The experimental spread of p*K*_a values is from 8.95 to 11.12; if we neglect PD (p*K*_a 11.12) the spread narrows to less than 1 p*K*_a unit (from 8.95 to 9.92). Both theories incorrectly predict DEA is more basic than MEA and NH₃, and the orders are wrong. The three candidates with the highest p*K*_a values (PD, PZ and EN) are correctly predicted by both theories, but again in the wrong order. No further discussion is warranted.

As we have also obtained optimized carbamic acid, as well as carbamate, structures, carbamic acid p*K*_a values were calculated. Even though the absolute p*K*_a values for the acid derivatives will only be qualitatively useful, the chemical resonance shown in Scheme 3 suggests the stability of the carbamic acid derivative can be assessed through direct comparison of the acid p*K*_a's, with a higher value indicative of greater resonance stabilization and a more favourable amine–acid interaction within the carbamic acid group. There are no reliable values for carbamic acid p*K*_a's in the open literature, so comparisons with experiment cannot be made in this instance. A plot of the theoretical carbamic acid p*K*_a values is shown in Fig. 4.

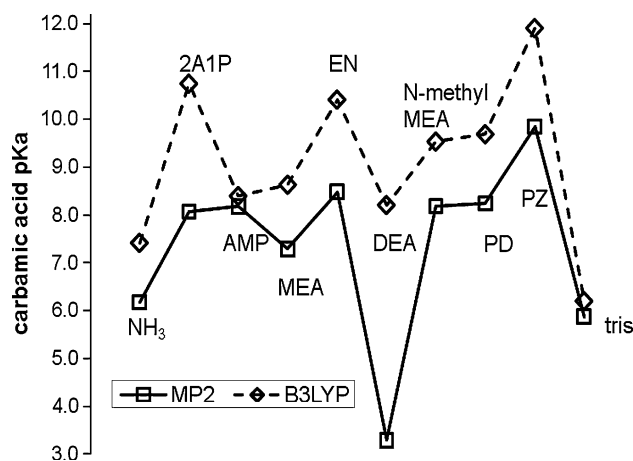


Fig. 4 p*K*_a values calculated for the carbamic acid derivatives of the capture amines investigated

According to our criteria of assessment outlined above, at the MP2 level PZ forms a stable acid capture derivative (high p*K*_a), and the acid capture derivatives of PD, *N*-methylMEA, 2A1P, AMP and EN are of comparable stability. The acid derivatives of MEA and NH₃ are slightly less stable, whereas those of DEA and tris are considerably less stable. At the B3LYP level, the results suggest tris, NH₃ and DEA will have less stable acid capture

derivatives, whereas PZ, EN and 2A1P will need larger heats of regeneration because of more stable acid capture derivatives. The results which are seemingly in conflict with the broad experimental consensus are those for DEA (suggested instability) and AMP (enhanced stability). While it is not inconceivable that the acid derivative of DEA could be less stable relative to the corresponding derivatives of other reagents studied, this theoretical anomaly can be readily explained by the formation of a highly stable carbamate or conjugate base. That is, the most stable carbamate conformer orients the hydroxyethyl –OH ‘arms’ to form two strong hydrogen bonds to the anionic –CO₂ group, in contrast to the most stable acid form (at both levels of theory) for which there is an intramolecular hydrogen bond between the hydroxyethyl OH-groups, i.e., no hydrogen bonding with the carbonyl group of the carbamic acid functionality. This gives rise to a low pK_a value. On the other hand, the seemingly high predicted stability of the AMP acid derivative is inconsistent with literature experimental findings, i.e., AMP is considered a “sterically hindered” amine [39] for which there is no available experimental data for the existence of its carbamate or carbamic acid derivatives. In this case the theory could be correct, especially if the derivative (carbamate or carbamic acid) forms readily in solution, but then hydrolyses rapidly to form bicarbonate as a result of other favourable factors. This point will be revisited in ensuing sections.

CO₂ capture reactions

The following discussion concerns equilibria 2 and 4 given in Scheme 1. Reaction 2 leads directly to carbamate formation, which is a possible reaction pathway only for 1°- and 2°-amine. A plot of ΔG_{aq} for this reaction calculated at both levels of theory is shown in Fig. 5¹ (top). With the exception of DEA (slightly exoergic), the MP2 ΔG_{aq} values are all endoergic. The B3LYP results are also endoergic, with the exceptions of EN, PD and PZ. Both levels of theory identify AMP and tris, the sterically hindered amines, as poor performers, consistent with the lack of experimental evidence for the existence of their carbamates or carbamic acids. EN, the heterocycles PD and PZ, and MEA, are predicted by both levels of theory to perform well in this regard, and this is certainly the experience of our (and other) laboratories. Surprisingly, MP2 predicts DEA will out-perform all other amines.

¹ The amount by which the B3LYP/6-31++G(d,p) free energies of reactions for 2 and 3 (Scheme 1) should be scaled is unclear; we have assumed the difference in the values predicted for NH₃ should provide a good estimate. For reaction 2, $\Delta G_{298.15}$ (MP2-B3LYP) = 21.6 kJ/mol. For reaction 3, $\Delta G_{298.15}$ (MP2-B3LYP) = 3.3 kJ/mol. No correction is necessary for reaction 3, as the difference suggests any error is within the accuracy of the calculation.

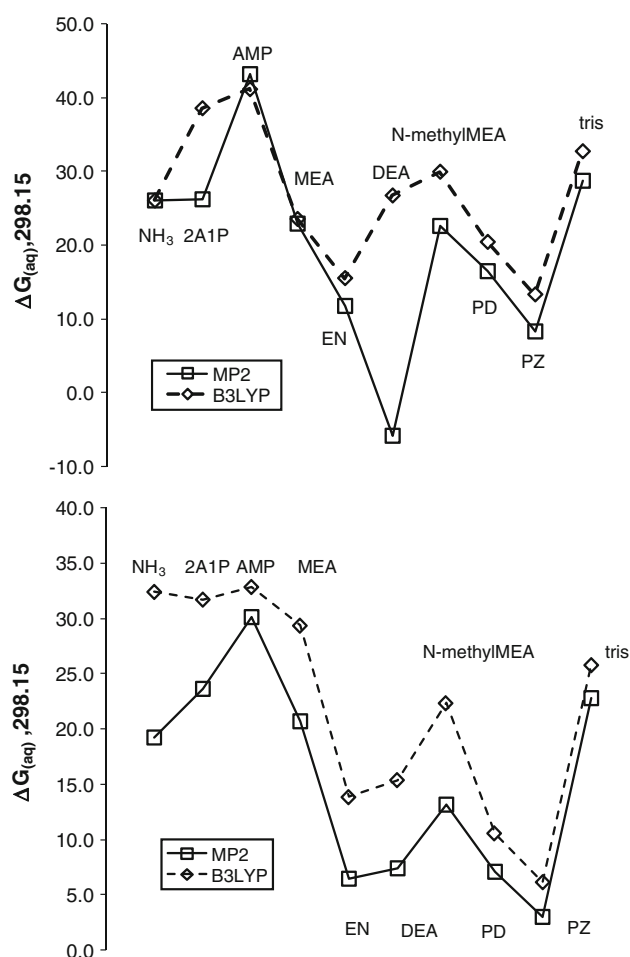


Fig. 5 MP2 and B3LYP ΔG_{aq} (kJ/mol) accompanying aqueous CO₂ capture. *Top*: carbamate formation, Scheme 1 reaction 2. B3LYP free energy values in the *top graph* adjusted by +21.6 kJ/mol. *Bottom*: bicarbonate formation, Scheme 1 reaction 4. B3LYP free energy values in the *bottom graph* adjusted by +38.1 kJ/mol

The ΔG_{aq} values associated with CO₂ capture to form bicarbonate have also been evaluated (reaction 4, Scheme 1). Once again the B3LYP results are uniformly exoergic and the MP2 results uniformly endoergic. Both theories agree on the comparative performance of the amines, however, for any given amine the magnitudes of the B3LYP and MP2 ΔG_{aq} are significantly different. The source of this discrepancy was located after calculating the sum of the aqueous free energies of formation of H₂O and CO₂, which was then subtracted from the aqueous free energy of formation of HCO₃⁻ for both theories; the difference between the MP2 and B3LYP values was found to be 38.2 kJ (i.e., HCO₃⁻ is more stable than H₂O plus CO₂ at the MP2 level). This difference is systematic in the MP2 ΔG_{aq} values, so the B3LYP values in Fig. 5 (bottom) are adjusted by this amount (see footnote 1). Perhaps the most surprising aspect of the ΔG_{aq} of the bicarbonate capture pathway is that the same high-performing carbamate

formers (the heterocycles, EN, DEA, MEA) are also represented amongst the high-performing bicarbonate-forming reagents. In contrast, NH_3 , AMP and tris (the latter two are sterically hindered) are poor performers. This is consistent with a correlation between amine $\text{p}K_{\text{a}}$ and the OH^- -catalysis pathway (i.e., the amines with high $\text{p}K_{\text{a}}$ have more negative reaction free energies). Overall, the results to this point are at least qualitatively consistent with reported experimental observations.

Carbamate hydrolysis

The ΔG_{aq} values for the carbamate hydrolysis reaction (Scheme 1, reaction 3) are shown in Fig. 6. Carbamate hydrolysis is almost as important from a process perspective as the CO_2 capture reactions, and we seek reagents which react quickly with CO_2 via reaction 2 (Scheme 1) but which hydrolyse to form the bicarbonate product, as this pathway is associated with a lower heat of regeneration. The direct (or carbamate) pathway to CO_2 capture (reaction 2) consumes two molecules of amine, whereas the indirect pathway (reaction 4, Scheme 1) only consumes a single amine molecule; carbamate hydrolysis regenerates the second amine molecule consumed by the direct pathway. MP2 predicts that the ΔG_{aq} values are positive but close to zero, with the exceptions of AMP, PD and *N*-methylMEA for which the free energy change is slightly negative. B3LYP results favour a slightly exoergic reaction. The heterocycle PD performs better than PZ at both levels of theory (carbamate prone to hydrolysis), and MEA and EN perform poorly. B3LYP predicts the carbamate derivative of NH_3 is less prone to hydrolysis than the MP2 results suggest. DEA has the most hydrolysis-susceptible carbamate according to B3LYP, whereas MP2 predicts it

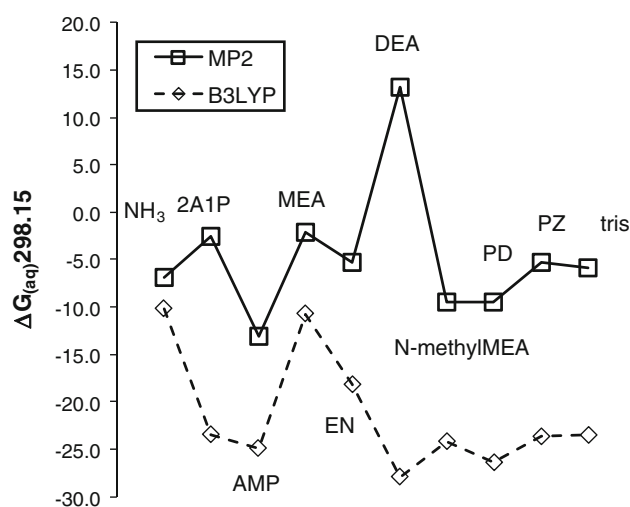


Fig. 6 ΔG_{aq} (kJ/mol) for carbamate hydrolysis (Scheme 1, reaction 3)

has the most stable carbamate; this discrepancy cannot be resolved at this time. The results for sterically hindered amines point to direct formation of hydrolysis-prone carbamates for these reagents.

Equilibrium constants

The computed values for the equilibrium constants for reactions 2–4 (see Scheme 1) appear in Table S3 of the supporting information. For equilibria 2–4, an ideal capture amine will have large values for K_2 through K_4 (equilibrium favouring the right-hand side). Both theories predict PZ, PD and EN will be high performers, while also agreeing on poor performance for AMP and 2A1P. MEA ranks towards the middle of the solvents investigated, chiefly due to its value for K_3 (which lies to the left, and concurs with experimental findings of a stable carbamate for this reagent). Due to the magnitude of the errors in the ΔG_{soln} values, the K_{eq} values shown in Table S3 are useful for inter-amine comparison only.

Analysis of overall changes in ΔG_{soln} for reactions 2–4 have been performed in order to investigate any changes in volatility and/or viscosity, which may occur during the capture process. For the purpose of this discussion, we define $\Delta(\Delta G_{\text{soln}})$ as:

$$\Delta(\Delta G_{\text{soln}}) = \sum_i n_i \Delta G_{i,\text{soln}}(\text{products}) - \sum_j n_j \Delta G_{j,\text{soln}}(\text{reactants}) \quad (2)$$

$\Delta(\Delta G_{\text{soln}})$ values for the CO_2 capture equilibria 2 and 4 (Scheme 1) are large and negative when weighted according to solution phase conformer populations at both levels of theory, suggesting a large decrease in volatility and/or an increase in viscosity during capture. This is not surprising considering the volatile molecule CO_2 is converted into a non-volatile ion in both reactions. As previously noted, it is difficult to separate decreases in volatility from viscosity increases, however, relative values at each level of theory might be used to qualitatively ascertain which solvents are likely to have increased viscosity after CO_2 loading. A plot of relative $\Delta(\Delta G_{\text{soln}})$ changes for these reactions can be found in Supporting Information (Fig. S1). DEA, tris and AMP have the most favourable $\Delta(\Delta G_{\text{soln}})$ changes, whereas capture solutions containing heterocycles, MEA, and EN will have increased viscosity. NH_3 appears to have the most unfavourable $\Delta(\Delta G_{\text{soln}})$ changes for reactions 2–4, however, this can be attributed to sequestration of volatile NH_3 molecules as ammonium ions and not necessarily viscosity increases. Formation of ammonium ions upon reaction is somewhat beneficial as ammonia slip (loss of NH_3 from the reactor to the environment) is problematic in any NH_3/CO_2 process.

Concerning capture reaction 4 (Scheme 1), tris is by far the best performer (the least negative $\Delta(\Delta G_{\text{soln}})$ followed

by DEA and AMP. This is consistent with the structures of these capture reagents, for which the hydrophobic parts of the hydroxyalkyl groups will disrupt the conductor-like solvent structure.

The hydrolysis of carbamate to yield bicarbonate (reaction 3, Scheme 1) conserves the number of ions in solution, hence the values predicted by the theory are not as large and negative, and in the case of NH_3 , the value is actually positive. The heterocycles and EN appear to be the best performers for carbamate hydrolysis, although there is little doubt the volatility of PD contributes to a less negative $\Delta(\Delta G_{\text{soln}})$ relative to the other reagents.

Conclusions

Two modest levels of computational theory (B3LYP/6-31++G(d,p) and MP2/6-311++G(d,p)) have been used to investigate aspects of CO_2 capture by aqueous amines. In particular, the theories correctly predict (i) the enhanced capture performance of heterocycles, which are currently under investigation in a number of laboratories, and (ii) poor performance for reagents such as NH_3 and sterically hindered amines. None of the results for AMP or tris (sterically hindered amines) indicate that they do not form carbamates in solution.

Supporting information

Optimized gas phase geometries at both levels of theory (B3LYP/6-31++G(d,p) and MP2/6-311++G(d,p)) for all amines, protonated amines, carbamates and carbamic acid structures used to derive averaged solution free energies. Figure S1: Plot of $\Delta(\Delta G_{\text{soln}})$ values for the capture reactions (2, 4) in Scheme 1. Table S1: Theoretical and experimental gas phase basicities and proton affinities for simple amines. Table S2: IEF-PCM UA HF/6-31G(d) solvation free energies for simple ions and molecules. Table S3: Aqueous equilibrium constants from MP2/6-311++G(d,p) and B3LYP/6-31++G(d,p) computations.

Acknowledgments PJ and MIA would like to thank the Coal Portfolio and the Computational and Simulation Sciences Transformed Capability Platform (CSS-TCP) c/o Dr John Taylor, Centre for Mathematical and Information Sciences (CMIS, CSIRO) for financial support, and Dr Robert Bell (HPSCC, CSIRO) for technical support.

Open Access This article is distributed under the terms of the Creative Commons Attribution Noncommercial License which permits any noncommercial use, distribution, and reproduction in any medium, provided the original author(s) and source are credited.

References

- Brennan ST (2009) Workshop on CO_2 sequestration. In: Proceedings of the 34th international conference on clean coal and fuel systems. 31 May–5 June, Clearwater, FL
- Netherlands Environmental Assessment Agency Report. Global CO_2 emissions annual increase halves in 2008. <http://www.pbl.nl/en/publications/2009>
- Garnaut R (2008) The Garnaut climate change review: final report. Cambridge University Press, New York, p 29
- Chi S, Rochelle G (2002) *Ind Eng Chem Res* 41:4178–4186
- Rooney PC, DuPart MS, Bacon TR (1998) *Hydrocarbon Proc. July*:109–113
- Attalla MI, Azzi M (2010) Environmental impacts of atmospheric emissions from amine-based post combustion CO_2 capture. IE-AGHG workshop on the environmental impacts of amine emission during post-combustion capture. February 16, Oslo, Norway
- Wang PG, Xian M, Tang X, Wu X, Wen Z, Cai T, Janczuk AJ (2002) *Chem Rev* 102:1091–1134
- McCann N, Maeder M, Attalla M (2008) *Ind Eng Chem Res* 47:2002–2009
- Yang Q, Bown M, Ali A, Winkler D, Puxty G, Attalla M (2009) *Energy Proc* 1:955–962
- Puxty G, Rowland R, Allport A, Attalla M, Yang Q, Bown M, Burns R, Maeder M (2009) *Environ Sci Technol* 43:6427–6433
- Jackson P, Robinson K, Puxty G, Attalla M (2009) *Energy Proc* 1:985–994
- Rowland R, Puxty G, Attalla M (2009) A comparison of carbon dioxide absorption rates between ethanolamine and ammonia. Chemeca 2009, 27–30 September, Perth, Australia
- For details of the Munmorah, Tarong, Gaobeideng and Loy Yang pilot PCC plants, see: <http://www.newgencoal.com.au/>, <http://www.asiapacificpartnership.org/english/default.aspx>, and <http://new.dpi.vic.gov.au/energy>
- Cramer CJ, Truhlar DG (1999) *Chem Rev* 99:2161–2200
- da Silva EF, Svendsen HF (2006) *Ind Eng Chem Res* 45:2497–2504
- Schmidt MW, Baldrige KK, Boatz JA, Elbert ST, Gordon MS, Jensen JH, Koseki S, Matsunaga N, Nguyen KA, Su SJ, Windus TL, Dupuis M, Montgomery JA (1993) *J Comput Chem* 14:1347–1363
- GAMESS Userguide, 4th October 2007, Section 4: further information, p 110
- Bode BM, Gordon MS (1998) *J Mol Graph Model* 16:133–138
- Scott AP, Radom L (1996) *J Phys Chem* 100:16502–16513
- Lias SG, Bartmess JE (2008) Gas phase ion thermochemistry. <http://webbook.nist.gov/chemistry/ion/>
- Sousa SF, Fernandes PA, Ramos MJ (2007) *J Phys Chem A* 111:10439–10452
- Barone V, Cossi M, Tomasi J (1997) *J Chem Phys* 107:3210–3221
- Cossi M, Barone V, Cammi R, Tomasi J (1996) *Chem Phys Lett* 255:327–335
- Frisch MJ, Trucks GW, Schlegel HB, Scuseria GE, Robb MA, Cheeseman JR, Montgomery JA Jr, Vreven T, Kudin KN, Burant JC, Millam JM, Iyengar SS, Tomasi J, Barone V, Mennucci B, Cossi M, Scalmani G, Rega N, Petersson GA, Nakatsuji H, Hada M, Ehara M, Toyota K, Fukuda R, Hasegawa J, Ishida M, Nakajima T, Honda Y, Kitao O, Nakai H, Klene M, Li X, Knox JE, Hratchian HP, Cross JB, Bakken V, Adamo C, Jaramillo J, Gomperts R, Stratmann RE, Yazyev O, Austin AJ, Cammi R, Pomelli C, Ochterski JW, Ayala PY, Morokuma K, Voth GA, Salvador P, Dannenberg JJ, Zakrzewski VG, Dapprich S, Daniels AD, Strain MC, Farkas O, Malick DK, Rabuck AD, Raghavachari K, Foresman JB, Ortiz JV, Cui Q, Baboul AG, Clifford S,

- Cioslowski J, Stefanov BB, Liu G, Liashenko A, Piskorz P, Komaromi I, Martin RL, Fox DJ, Keith T, Al-Laham MA, Peng CY, Nanayakkara A, Challacombe M, Gill PMW, Johnson B, Chen W, Wong MW, Gonzalez C, Pople JA (2004) Gaussian 03, Revision C.02. Gaussian Inc, Wallingford, CT
25. Schüürmann G, Cossi M, Barone V, Tomasi J (1998) *J Phys Chem A* 102:6706–6712
 26. Kawazuishi K, Prausnitz J (1987) *Ind Eng Chem Res* 26:1482–1485
 27. Kelly CP, Cramer CJ, Truhlar DG (2006) *J Phys Chem B* 110:16066–16081
 28. Bryantsev VS, Diallo MS, Goddard WA III (2008) *J Phys Chem B* 112:9709–9719
 29. Kelly CP, Cramer CJ, Truhlar DG (2006) *J Phys Chem A* 110:2493–2499
 30. Bouchoux G (2007) *Mass Spectrom Rev* 26:775–835
 31. Karpas Z (1992) *Struct Chem* 3:139–141
 32. DaSilva EF (2005) *J Phys Chem A* 109:1603–1607
 33. Blackburne ID, Katritzky AR, Takeuchi Y (1975) *Acc Chem Res* 8:300–306
 34. Sunner JA, Kulatunga R, Kebarle P (1986) *Anal Chem* 58:1312–1316
 35. Jiang H, Zhang S, Xu Y (2009) *Afr J Pure Appl Chem* 3:126–130
 36. Marcus Y (1986) *J Chem Soc Faraday Trans 1*(82):233–242
 37. da Silva EF, Svendsen HF (2003) *Ind Eng Chem Res* 42:4414–4421
 38. Dissociation constants of organic acids and bases. In: Lide DR (ed) *Handbook of chemistry and physics*, 90th edn (Internet Version 2010). CRC Press, Taylor and Francis, Boca Raton, FL
 39. Sartori G, Savage DW (1983) *Ind Eng Chem Fundam* 22:239–249